International Journal of Precision Engineering and Manufacturing-Green Technology (2019) 6:415–432
https://doi.org/10.1007/s40684-019-00072-x

Online ISSN 2198-0810
Print ISSN 2288-6206

REGULAR PAPER

Experimental Investigation on Cryogenic Assisted Abrasive Water Jet Machining of Aluminium Alloy

Yuvaraj Natarajan[1] · Pradeep Kumar Murugasen[2] · Lenin Raj Sundarajan[3] · Rajadurai Arunachalam[3]

Received: 23 February 2018 / Revised: 26 August 2018 / Accepted: 4 September 2018 / Published online: 25 February 2019

Abstract

The purpose of the present investigation was to evaluate the abrasive water jet cutting performance by the application of a cryogenic liquid nitrogen jet in the cutting process. This technique was developed for improving the process capability of conventional abrasive water jet machining and enable a higher depth of cut and material removal rate, and better kerf profile and surface integrity. The experiments were conducted on AA5083-H32 aluminium alloy, using two different cutting methods, namely, abrasive water jet cutting and cryogenic assisted abrasive water jet cutting. Both cutting conditions were investigated by varying the water jet pressure, the abrasive mesh size and the abrasive water jet impact angle. Optical microscopy and Scanning Electron Microscope with Energy Dispersive X-ray Spectroscopy was used for studying the micro structure and morphology of the cut surfaces under both cutting conditions. There was an improvement in cutting performance features such as depth of penetration, material removal rate and kerf profile with the use of cryogenic assistance cutting approach. These results were produced due to the beneficial modification of erosion mechanism in the cutting zone as well as a reduction in particle embedment with the cut surface by about 56%.

Keywords Abrasive water jet · Cutting · Liquid nitrogen · Performance evaluation · Surface morphology

List of symbols

LN_2	Liquid nitrogen
AWJC	Abrasive water jet cutting
CAAWJC	Cryogenic assisted abrasive water jet cutting
EDS	Energy dispersive spectroscopy
SEM	Scanning electron microscope
DOP	Depth of penetration (mm)
MRR	Material removal rate (mm^3/min)
KTR	Kerf taper ratio
TR	Traverse rate
Pt	Maximum peak to valley height (μm)
P	Pressure (MPa)
MS	Abrasive mesh size (#)
JIA	Abrasive water jet impact angle (°)
Mg_2Al_3	Magnesium aluminide (β)
Ra	Average surface roughness (μm)

✉ Yuvaraj Natarajan
yuvaceg09@gmail.com

[1] Department of Mechanical Engineering, Vel Tech Rangarajan Dr. Sagunthala R&D Institute of Science and Technology, Chennai 600062, India

[2] Department of Mechanical Engineering, CEG Campus, Anna University, Chennai 600025, India

[3] Department of Production Technology, MIT Campus, Anna University, Chennai 600044, India

1 Introduction

Traditional machining processes like turning, drilling, and milling use a sharp edged cutting tool and the material from the workpiece is removed by shear deformation. However, these processes have certain restrictions in machining high strength materials. Cutting tools, harder than the workpiece, are required. The volume of heat developed during the machining is also high. This triggers the need for sophisticated machining processes for machining of different materials. Such processes can produce improved surface finish, and complex and intricate profiles. Among the machining processes, abrasive water jet cutting (AWJC) is used for smaller heat affected zones with less thermal stress acting on the workpiece, and the ability to cut different kinds of materials [1]. In AWJC, material removal takes place through the erosion process. A detailed description of this process can be seen in the relevant literature [2, 3]. AWJC has some limitations despite being well established. The limitations include the generation of a higher volume of secondary wastage

following machining, and of heat developed at the primary impact zone, abrasive contamination, striation formation, rough quality surface and low energy transfer efficiency from the nozzle to the workpiece, which cause a low depth of cut and material removal rate. Due to such limitations, the use of this process was very limited in industries.

Some researchers have made attempts at improvements in the cutting performance of AWJ through various techniques such as thermally enhanced AWJ cutting [4], recycling of abrasives [5], changing the abrasive mesh size [6–9] and the abrasive water jet impact angle [7–10], and using unconventional abrasives [11]. Recently, Yuvaraj and Kumar [7–9] confirmed the achievement of better cutting performance in aluminium alloy and die steel with improved surface quality through the employment of oblique jet impact angles. This happened due to the existence of a threshold level of abrasive particle energy caused by oblique jet impact angles. However, in the present era, industries are looking for high surface quality, absence of burr formation and reduction in kerf taper effect, which can improve the productivity level. Therefore, researchers have been made attempts at improving the machining process, through use of cryogenic assisted machining.

Recently, cryogenic assisted machining was used for machining materials of a wide range. Researchers used cryogenic assisted machining in different areas like turning, milling, drilling, and grinding for machining different materials. Cryogenic assisted machining is a safe environmental alternative approach for improving cutting performance through enhancement of the properties of the target material at low temperature [12]. Most researchers used liquid nitrogen (LN_2) in different machining processes, considering that it liquefies by cooling to – 196 °C. It offers an easy material removal rate, with no harmful effects, is non-corrosive, non-flammable, easy to dispose in the environment, and improves surface integrity through the controllable phase changes in the target material at low temperature [13, 14]. This technique can be applied also to the abrasive water jet (AWJ) for machining different kinds of materials, which are widely used in aerospace, automotive and marine applications. Previous research in turning, drilling and milling processes has reported a substantial benefit from cryogenic assisted machining in the reduction in cutting forces, improvement in surface roughness and reduction in tool wear, and help in producing a good surface roughness, faster material removal rate, less machining time, better dimensional accuracy and absence of burr formation [15–17]. They have indicated that cryogenic cooling, using LN_2 as the coolant, was an environment friendly alternative method for improving machining performance.

Truchot et al. [18] developed the cryogenic water jet technique for processing bio-materials. They found the cutting efficiency of the cryogenic process as better than that of the pure water jet. Gradeen et al. [19] studied the cryogenic abrasive jet machining of polydimethylsiloxane at different temperatures. The result showed the cutting region getting cooled to about – 178 °C, and consequently, increasing the material removal rate through the brittle behaviour erosion process. Later, they investigated the same machining process in polytetrafluoroethylene, high carbon steel and polydimethylsiloxane. The result showed an increase in the erosion rate and reduction in particle embedding in the machined surface through the employment of a cryogenic liquid with various temperatures in the abrasive jet machining process [20]. Getu et al. [21] studied the machining of PDMS using cryogenic assisted abrasive jet machining. This process cooled the target material below its glass transition temperature, thereby enabling material removal via brittle erosion mechanisms. Urbanovich et al. [22] have reported increase in the erosion rate of the steel by about 1.7 times under cryogenic cooling over abrasive jet erosion at room temperature.

Getu et al. [23] carried out cryogenically assisted abrasive jet micromachining of different polymers, namely, PDMS, ABS and PTFE. They observed the use of LN_2 cooling causing brittle erosion in PDMS, and found a reduction in particle embedding in the machined surface. Spur et al. [24] developed a dry ice blasting (CO_2) technique for the removal of soil and paint from aluminium–magnesium alloys. The results indicated a complete removal of contamination. Liu et al. [25] studied the enhancement of ultra-high pressure technology with LN_2 cryogenic jets. The results reported a completely safe environment due to the absence of any residue after the machining operations. Muju and Pathak [26] reported an increase in the erosion rate of the glass at low temperature by the use of cryogenic abrasive jet machining. The result showed an increase in the erosion rate compared to that at room temperature. Kim et al. [27] found large advantages from cryogenic cutting technology including reduction in secondary wastages, particle contamination, and modifications in the failure mode of the target material.

Based on the previous literatures, a few researchers made attempts at using cryogenics in different machining processes. They also developed the use of a cryogenic system in an abrasive water jet with modified conditions, such as ice jet machining, and abrasive cryogenic jets with replacement of conventional abrasives. These conditions helped improvement in the surface cleaning technology, but not the cutting performance [28]. Later, Yuvaraj and Kumar [29] developed a cryogenic assisted abrasive water jet machining process for investigation of surface integrity of the machined surface. The result indicated an improvement in the surface integrity of the cryogenic assisted machining process compared to the AWJ process at room temperature. However, there was no attempt from the earlier researchers in the assessment

of the performance characteristics under cryogenic assisted abrasive water jet cutting (CAAWJC) process.

The main aim of this investigation was to conduct the CAAWJC of aluminium alloy, namely, AA5083-H32, which is used for enhancing the performance characteristics such as depth of penetration, material removal rate, kerf taper ratio, surface roughness and the surface quality of the target material. Further, this aluminium alloy was chosen as being sensitive to machining by other machining processes. This is due to its susceptibility to stress corrosion cracking and fatigue crack growth, when exposed to elevated temperatures in the range of 50–200 °C, or for a very long time at room temperature, and when the magnesium (Mg) content is more than 3% in the AA 5xxx series of aluminium alloys [30–33]. In the CAAWJC process, the cryogenic liquid is used for cooling the cutting zone, allowing the material removal with an appreciable reduction in ductility, and increase in the hardness at the cutting zone.

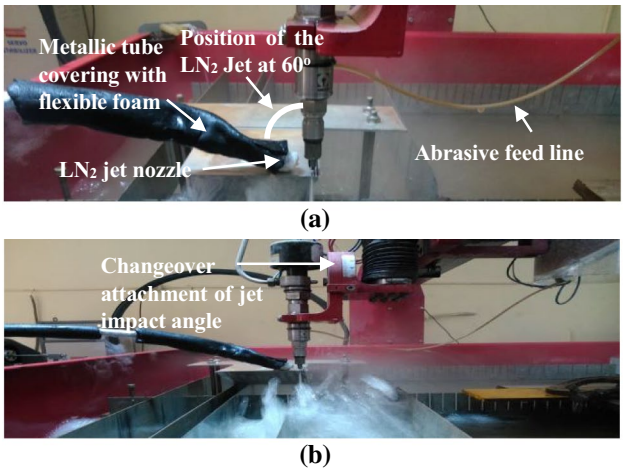

Fig. 2 Enlarged view of the cryogenic assisted jet machining experimental setup, **a** with normal abrasive water jet impact angle, **b** with an oblique abrasive water jet impact angle

2 Experimental Work

Experimental work was done in the Abrasive water jet machine OMAX MAXIEM 1515 which has a special provision for a change-over attachment of the abrasive water jet impact angle/jet impact angle. The schematic layout of the CAAWJC process is shown in Fig. 1. The enlarged view of the normal and oblique abrasive water jet impact angles setup for CAAWJC is shown in Fig. 2. In the CAAWJC process, the LN_2 was injected into the cutting zone and the LN_2 jet pressure, flow rate and the LN_2 jet angle were carefully chosen, to ensure avoidance of the formation of ice particles in the cutting zone and the deflection of the AWJ. The LN_2 jet nozzle was positioned beside the abrasive water jet focusing nozzle with its centre axis inclined approximately 60° from that of the nozzle. This optimum angle minimised the interruption of the flow of the abrasive water jet, and makes coverage uniform in the cutting zone. It also provides sufficient cooling to the abrasive water jet mixture. This cooling happens abrasive particles in the jet getting frequently hardened and subsequently involved in the machining action with higher efficiency. Compressed air was used for delivery

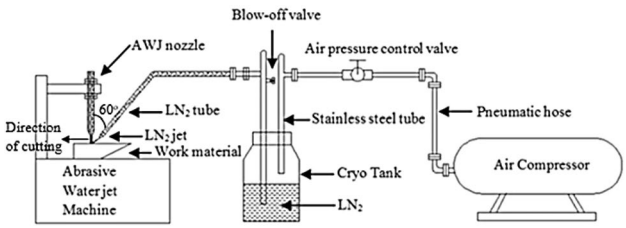

Fig. 1 Schematic layout for cryogenic assisted abrasive water jet machining setup

of LN_2 from the cryo tank into the cutting zone through the LN_2 nozzle. A blow-off valve was used in the LN_2 transfer tube, which delivered the LN_2 at the desired pressure for avoiding the waste and contamination of LN_2. In addition to this, the LN_2 jet pressure could be increased beyond 4–5 bar which would increase freezing in the delivery line of the LN_2 jet [17] as well as water jet due to the increase in flow rate of the LN_2 rate. This caused production of the fine ice particles and mist in the machining zone making the process a serious. Also, its disposal is easy with a small expansion ratio to the environment. Using the METRAVI digital non-contact type IR thermometer (model: MT-8), the temperature was measured and found to be in the range of – 50 to 1000 °C. The dual light sighting indicated the diameter of the target at the machining zone whose temperature was measured.

In this study, AA5083-H32 aluminium alloy has been chosen as the target material. It is highly enriched with 5.31% of Mg and widely used in automotive and marine applications. This alloy is prone to cracking, and reduction in strength and hardness when the operating temperature exceeds 65 °C. It also performs better under low temperature. It is difficult to machine through use of other manufacturing processes due to its poor machinability, as reported by Totten et al [34]. All the experiments were conducted on the wedge shaped [35] AA 5083-H32 aluminium alloy, with a thickness of 64.065 mm, as shown in Fig. 3. The wedge shaped workpiece was specifically chosen for the visual examination of the depth of penetration, considering the variations in the depth of penetration under different sets of parameter combinations [7]. The abrasive water jet splashes towards the side of the machine operator, clearly indicating to the operator beyond the point beyond which the AWJ cannot penetrate the workpiece, for the corresponding

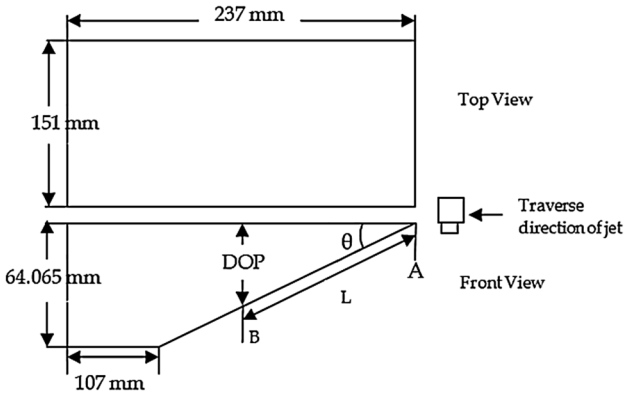

Fig. 3 Wedge shaped AA5083-H32 workpiece

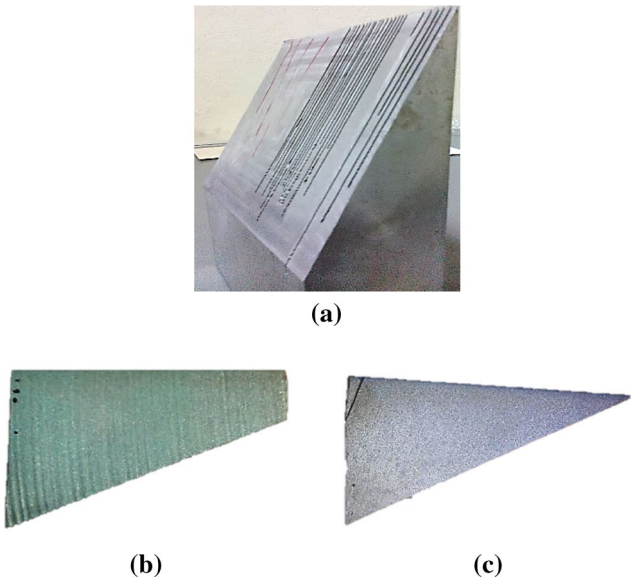

Fig. 4 Photographs of the machined aluminium alloy, **a** kerf profile, **b** AWJC kerf wall cut surface, **c** CAAWJC kerf wall cut surface

experimental parameter combinations. The supply of LN_2 into the cutting zone is very limited during the cutting operations. It is not also to the entire cutting length. The supply is done only where the deflection of the jet is indicated by the operator. It is continuous later until the introduction of a further deflection of the jet. This optimum level of condition has been adopted in this study, for reducing the consumption of LN_2 and the cost.

For this experimental study, the pressure, garnet (abrasive) mesh size and the abrasive water jet impact angle were the variable process parameters. The cutting process parameters and their levels are shown in Table 1. A standard orthogonal array of L_9 was chosen on the basis of the factors and their levels. In this research work, the depth of penetration, the material removal rate, kerf taper ratio, roughness, and abrasive contamination were considered as the parameters of the cutting performance of the AWJC and CAAWJC processes. Figure 4 shows the photographs of the kerf wall cut surfaces under AWJC and CAAWJC.

The following equation was used for the calculation of the depth of penetration (DOP):

$$DOP = L \times \sin\theta, \tag{1}$$

where, L is the slant length in mm and θ is the angle (°).

Material removal rate (MRR) is the important parameter, which has a direct effect on productivity. It is defined by the volume of material that can be removed during a certain period, and is expressed in mm^3/min. The MRR was measured using the following equation:

$$MRR = DOP \times AKW \times TR, \tag{2}$$

where, AKW is the average kerf width in mm, and TR is the traverse rate (mm/min).

The kerf width values were measured using a tool maker microscope with the least count of 0.005 mm and magnification of 10×.

Table 1 Experimental cutting conditions

Process parameters	Levels		
	Level 1	Level 2	Level 3
Pressure (P) (MPa)	100	125	150
Abrasive mesh size (MS) (#)	80	100	120
Jet impact angle (JIA) (°)	70	80	90
Traverse rate (mm/min)	15		
Focusing nozzle diameter (mm)	0.7		
Orifice diameter (mm)	0.35		
Stand-off distance (mm)	3		
LN_2 jet pressure (bar)	4		
LN_2 jet spray angle	60° from the AWJ nozzle		
AWJ nozzle direction	Forward type		
LN_2 flow rate (l/min)	0.54		

In this study, the kerf taper ratio (KTR) was the desirable parameter which determined the quality and performance of AWJ using the following equation [2].

$$KTR = b_T/b_B, \tag{3}$$

where, b_T is the average top kerf width in mm, and b_B is the average bottom kerf width in mm.

The average top kerf width and bottom kerf width were obtained from the measurements taken at three different locations of the target material. The following procedure was considered for the measurement of the kerf width [7, 9].

- For the measurement of kerf taper, the traverse length of the jet over the target material was fixed. The fixed length was taken as 70 mm. The points on the top and bottom cut surfaces were marked at three locations for the mean value.
- To ensure lower volume of materials and cost, the above measurements were taken into account during the experimental work.

Surface roughness was measured using the surfcorder SE3500, Kosaka laboratory limited—Japan, with a traverse length of 4 mm, cut-off length of 0.8 mm and the probe head size of 2 µm. The average roughness values were measured at the upper kerf wall surfaces. In this study, the upper zone measured 2 mm from the top of the cut surface [36]. The characteristics of the 2D surface profile and 3D surface topography were obtained by using the Taylor Hobson Tally-Surf CCI profilometry equipment with a model of ISO 4287 series. The measurement was taken at 3 mm from the top cut surface with a magnification of 10×. In the 2D roughness profile and 3D surface topography, the horizontal axis constituted the focusing area of 3250 µm along the AWJ kerf wall cut surface direction, and the vertical axis constitutes the amplitude value of the surface roughness profile.

The microstructure was taken through the use of a metallurgical microscope-METSCOPE 1A with a magnification of 100×. The cut surfaces were polished by alumina on high napped polishing cloths. Then the polished surfaces were etched with 1% Hydrofluoric solution for less than 20 s. A Scanning electron microscopy (SEM) with Energy Dispersive X-ray Spectrometer (EDS) was used for studying the abrasive contamination (before cleaning operations) of the cut surfaces under AWJC and CAAWJC conditions. SEM micrographs were taken under the mode of secondary electron. The micro hardness values were measured using a micro hardness tester—Wolpert Group equipment with a load of 100 g ($HV_{0.1\,kg}$) and 10 s dwell time.

3 Results and Discussions

3.1 Effect of LN_2 Cooling on Depth of Penetration (DOP)

The percentage of improvement in the DOP due to the CAAWJC process compared to the AWJC process for different water jet pressures, abrasive mesh sizes and abrasive water jet impact angles in the cutting of AA5083-H32 aluminium alloy is shown in Table 2. Figure 5 shows the effect of LN_2 on the DOP with various combinations of abrasive mesh sizes and abrasive water jet impact angles.

Variations depend on three different water jet pressures with other fixed process parameters. Figure 5a–c, it shows increase in the DOP with an increase in the water jet pressure for different levels of the abrasive water jet impact angle, with an abrasive mesh size under the CAAWJC process. Achievement of the maximum penetration depth with a higher level of water jet pressure 150 MPa, abrasive mesh size of #80 with an abrasive water jet impact angle of 90° was seen as possible. The maximum DOP achievable with this combination was found to be 63.44 mm. This specific behaviour was feasible through reduction in particle embedding and fractured abrasives at the initial cutting zone, and maintaining the velocity of the coarser abrasive particles

Table 2 Variation of DOP values under AWJC and CAAWJC conditions

Ex. no	P/MPa	MS/#	JIA/(°)	AWJC Avg. DOP (mm)	CAAWJC Avg. DOP (mm)	% of improvement
1	100	80	70	35.93	42.62	16
2	100	100	80	43.54	45.43	4
3	100	120	90	43.68	46.02	5
4	125	80	80	44.83	51.98	14
5	125	100	90	41.01	48.66	16
6	125	120	70	34.52	36.25	5
7	150	80	90	43.15	63.44	32
8	150	100	70	38.90	49.48	21
9	150	120	80	42.61	46.82	9

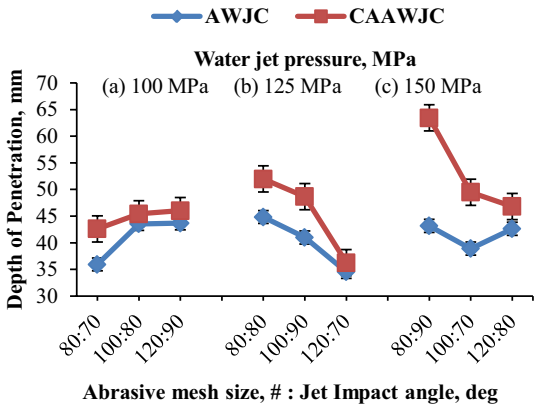

Fig. 5 Variation of depth of penetration under different experimental conditions, **a** 100 MPa, **b** 125 MPa, **c** 150 MPa

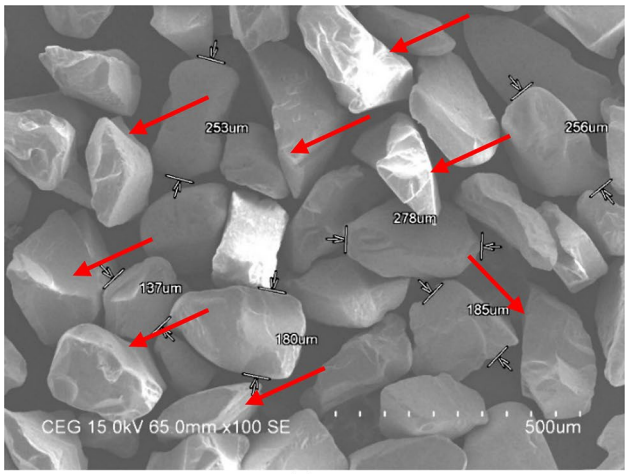

(a)

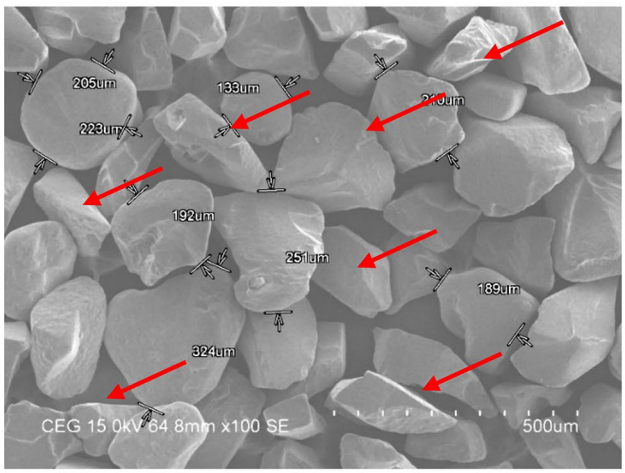

(b)

Fig. 6 Sharp edges of abrasives, **a** mesh size #80, **b** mesh size #100

effectively in the lower cutting region. Increase in the DOP with an increase in the water jet pressure could also be observed along with various combinations of mesh sizes of the abrasives and the abrasive water jet impact angle. As a result, larger kinetic energy was available for penetrating the material due to the shearing action of the abrasive particles, which showed improvement in the CAAWJC process. This cutting process allowed the cutting zone material with a reduction of ductility, and also increase in hardness, which helped reducing the particle embedding in the kerf wall cut surface. The hardened material restricted particle embedding in the cut surface over the soft condition of material at room temperature. In addition to this, the particles get hardened frequently with the LN_2 jet and produce a lower fracture at the harder surface. As a result, larger kinetic energy was available for disintegrating the target material, thereby increasing the DOP with the help of a smaller quantity of fractured abrasives. In the AWJC process, the ductility of the material remained unchanged, leading to production of the deformation followed by a fracture. More fractured abrasives were produced as a result of this. It is also noted that, the abrasive water jet impact angle of 90°, and the coarse abrasive particles with a higher water jet pressure result in a lower DOP. This inducement of deformation in the high impulse of the abrasive particles impact with the target material was observed, as also the yield of a low DOP with more fractured abrasives as a result.

The AWJC results indicated a water jet pressure of 125 MPa and 150 MPa, involving particle disintegration of a higher degree due to the higher impulse (critical energy) existing in the target material during the jet impact angle of 90°; there was a reduction in DOP as a result. In contrast, a water jet pressure of 100 MPa offered sufficient kinetic energy with less particle disintegration at the jet impact angle of 90° and produced a higher depth of penetration. The jet impact angle 90° produced a higher cutting force compared to the oblique jet impact angles. Ex. No. 5 and 7 indicate the abrasive mesh size as #100 and #80. There was an increase in the size of the abrasive particles with a decrease in decreasing the size of the particle mesh. Also, these particles contain sharp edges is shown in Fig. 6. A coarse size with sharp edges of the abrasive particles (#80 and #100) having a higher density with critical kinetic energy was produced due to the employment of jet impact angle of 90°. However, a water jet pressure of 150 MPa compensated for the energy of the disintegrated abrasive particles (#80) at jet impact angle of 90° and yielded a higher jet penetration over the Ex. No. 5.

It also revealed the cutting action of the abrasive particles, based on their density and shape. The coarser particles have more kinetic energy for cutting the material, and the ability to produce the maximum DOP [37]. The AWJC process offering higher DOP at a water jet pressure of 125 MPa, abrasive mesh size of #80 and abrasive water jet impact

angle of 80° were also seen, while the DOP was found to be 43.15 mm. This combined parameter setting could contribute to a reduction in the cutting force of the abrasive particles. However, it has sufficient kinetic energy to disintegrate the material with lower number of fractured abrasives and particle embedding, consequently increasing the DOP. The conclusion was that the influence of LN_2 cooling with other process parameters, namely, water jet pressure, abrasive water jet impact angle and abrasive mesh size, offered a higher DOP at a lower temperature than the erosion at room temperature, with improvement by 4–32% compared to the AWJC process. This particular result was realised through the reduction in particle embedding and fractured abrasives in the cutting process.

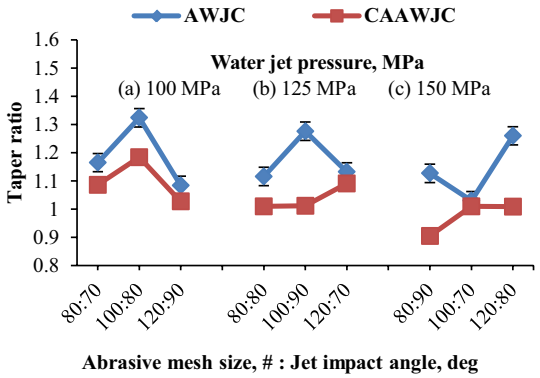

Fig. 7 Variation of taper ratio under different experimental conditions. **a** 100 MPa, **b** 125 MPa, **c** 150 MPa

3.2 Effect Of LN_2 Cooling on Kerf Taper Ratio

Table 3 shows the percentage reduction in the kerf taper ratio resulting from the CAAWJC process compared to the AWJC process for different water jet pressures, abrasive mesh sizes and abrasive water jet impact angles in the cutting of AA5083-H32 aluminium alloy. Variations in the kerf taper ratio seen during the cutting of aluminium alloy under AWJC and CAAWJC processes are shown in Fig. 7.

Figure 7a–c shows a decrease in the kerf taper ratio during the CAAWJC process for the various combinations of water jet pressure, abrasive mesh size and abrasive water jet impact angle. A lower kerf taper ratio was achieved with a water jet pressure of 150 MPa, abrasive water jet impact angle of 90° along with an abrasive mesh size of #80. This was possible through a comparison of the various levels of combinations. As a result, the minimum kerf taper ratio achievable with this combination was found to be 0.905. LN_2 was found to be more significant in the kerf taper ratio, irresepective of the thickness of the cutting material thickness and different levels of cutting parameter combinations. There was a loss of kinetic energy of the abrasive particles in the AWJC process in the abrasive water jet impact angle of 90° with high pressure, while there was an increase in the depth of penetration, and finally, became a non-linear kerf profile when abrasive mesh sizes of #80, #100 and #120 were used.

Oblique abrasive water jet impact angles could be seen as significant, when they interact with the lower water jet pressure. This result happens due to the cutting energy of abrasive particles, that should be retained throughout the cutting operation, which happened to be the effect of jet cooling on the target surface. Some times, a poor kerf taper ratio occurs in the AWJC process due to the disintegration of the abrasive particles and particle embedding in the cutting zone. This leads to deflection of the cutting direction of the AWJ, following an increase in the penetration depth, with the formation of a taper as a consequence. The cutting wear mode is more effective on the top and bottom of the kerf width causing a parallel kerf width in the cut surfaces. The cutting energy of abrasive particles should be retained throughout the cutting operation; this need araises due to the effect of the reduction in particle embedding and fractured abrasive particles under the CAAWJC process. As a result of this, the energy of the abrasive particles is retained at the

Table 3 Variation of taper ratio values under AWJC and CAAWJC conditions

Ex. no	P/MPa	MS/#	JIA/(°)	AWJC Avg. TR	CAAWJC Avg. TR	% of Reduction
1	100	80	70	1.165	1.086	7
2	100	100	80	1.324	1.186	11
3	100	120	90	1.082	1.027	5
4	125	80	80	1.116	1.010	10
5	125	100	90	1.276	1.012	21
6	125	120	70	1.132	1.091	4
7	150	80	90	1.127	0.905	20
8	150	100	70	1.030	1.001	2
9	150	120	80	1.260	1.009	20

lower cutting regions, and producing a smaller taper in the kerf profile. When this happens, no striations are found in the lower cutting region of the cut surface in the CAAWJC process. This is shown in Fig. 4c. The result also indicates an increase in the top kerf width for the higher pressure and the coarse abrasives (#80) due to the LN_2 cooling jet being more effective. Meanwhile, the low pressure of the AWJ has a positive influence on the top kerf width and bottom kerf width due to the capable CAAWJC, which offers less divergence at the entry and exit of the cut surface in the target material. The conclusion is that, the effect of LN_2 jet cooling reduces the kerf taper ratio by 2% to 21% in the CAAWJC process.

3.3 Effect of LN_2 Cooling on the Material Removal Rate (MRR)

Table 4 indicates the percentage improvement in the MRR in the CAAWJC process compared to the AWJC process for various water jet pressures, abrasive mesh sizes and abrasive water jet impact angles in the cutting of AA5083-H32 aluminium alloy. Figure 8 shows the effect of LN_2 cooling on the MRR with different combinations of abrasive mesh sizes and jet impact angles, which depend on three different water jet pressures.

Figure 8a–c shows an increase in the MRR arising from an increase in the water jet pressure for different levels of the abrasive mesh sizes and the abrasive water jet impact angles in the CAAWJC process. Achievement of a higher MRR with a higher level of water jet pressure of 150 MPa with an abrasive water jet impact angle of 90° and abrasive mesh size of #80 was seen in the experiment. The maximum achievable MRR with this combination was found to be 1474.980 mm^3/min. Consequently, the abrasive water jet impact angle at 90° with higher water jet pressure offers greater erosion while cutting, and removing large amounts of material from the target material during a certain period of time. The LN_2 cooling in the cutting process allowed the erosion process through a fine debris (micro cutting) rather than chip-like debris (microchips), and yielded a more efficient MRR. This chip-like debris is commonly produced in AWJC of aluminium alloy at room temperature [38]. The fine debris erosion process happened through reduction in ductility, and increase in the hardness of the cutting zone. This could cause an increase in the erosion rate due to the higher involvement of micro cutting action in the cutting zone through the prolongs of size and shape of the abrasives, which in turn increased the removal rate of material [39]. During the LN_2 jet cutting process, abrasive particles got hardened and sharpened; leading to the occurrence of frequent failures of material through the shearing action rather than the combined effects of shearing and deformation process. As result of this, higher MRR was observed. In contrast, the AWJC process generated a higher MRR at a lower water jet pressure, with the combined effect of the abrasive mesh size #100 and abrasive water jet impact angle of 80°. This specific result arose from the threshold energy of the abrasive water jet that occurred on the target material and produced a smaller particle disintegration. A similar trend

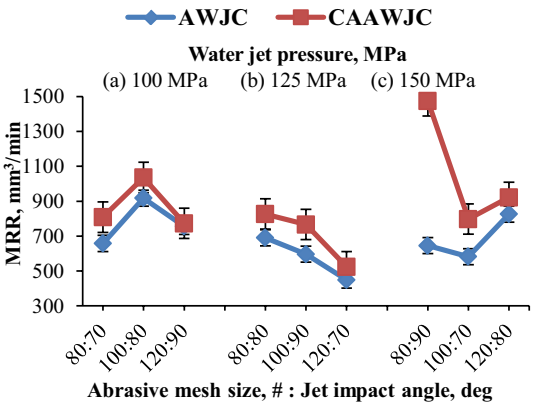

Fig. 8 Variation of material removal rate under different experimental conditions, **a** 100 MPa, **b** 125 MPa, **c** 150 MPa

Table 4 Variation of MRR values under AWJC and CAAWJC conditions

Ex no	P/MPa	MS/#	JIA/(°)	AWJC Avg. MRR (mm^3/min)	CAAWJCAvg. MRR (mm^3/min)	% of Improvement
1	100	80	70	657.519	808.715	19
2	100	100	80	917.395	1035.804	11
3	100	120	90	755.447	773.136	2
4	125	80	80	690.606	826.281	16
5	125	100	90	596.550	766.584	22
6	125	120	70	449.192	524.719	14
7	150	80	90	645.632	1474.980	56
8	150	100	70	582.041	797.865	27
9	150	120	80	825.782	922.036	10

of medium pressure with an abrasive water jet impact angle of 80° producing sufficient kinetic energy to erode the aluminium alloy was also observed. This combination enabled a higher material removal rate compared to the combined effect of the abrasive mesh size of #80 and abrasive water jet impact angle of 90° with a higher water jet pressure.

In the AWJC process, the oblique abrasive water jet impact angles produce a lower tangential cutting force than the normal abrasive water jet impact angle (90°). However, the oblique jet impact angles maintained the kinetic energy of the abrasive particles throughout the cutting operations with wide kerf entry. This was the effect of uniform distribution of particle energy. As a result, sufficient kinetic energy was maintained at the top and the lower cutting regions with a uniform kerf width, producing a better MRR. The CAAWJC results, showed the oblique abrasive water jet impact angle enabling a smaller material removal rate compared to the jet impact angle 90°. This was a consequence of the reduction in embedded abrasive particles, as the normal abrasive water jet impact angle on the AWJC process caused a larger disintegration of the abrasives due to the existing critical energy (high impulse) that exist. This level of particle disintegration caused a reduction in the erosion rate resulting from the occurrence of larger deflection of abrasive particles at a water jet pressure of 150 MPa and abrasive mesh size of #80 employed. As a result, there was removal of a smaller quantity of material from the target material. There was also the formation of striations in the lower cutting region of the cut surface in the AWJC process (Fig. 4b), attributed to the availability of lower kinetic energy in the lower cutting region by the fragmented abrasive particles. The role of LN_2 cooling, and the combined effect of the abrasive mesh size and abrasive water jet impact angles with water jet pressure, were found to be significant in MRR. The conclusion is that MRR increased by 2% to 56% in the CAAWJC process.

3.4 Effect Of LN_2 Cooling on Surface Roughness

Table 5 shows the percentage of reduction in the average surface roughness arising out of the CAAWJC process compared to the AWJC process for different water jet pressures, abrasive mesh sizes and abrasive water jet impact angles in the cutting of AA5083-H32 aluminium alloy. The variations in the average surface roughness during the cutting of the aluminium alloy under AWJC and CAAWJC processes is shown in Fig. 9.

In this experimental study, surface roughness was measured at 2 mm from the top of the cut surface with respect to the traverse direction of the jet. Among the various combinations of cutting parameters, LN_2 jet cooling was seen as more significant. This occurred as a result of LN_2 jet cooling, which in turn increased the hardness of the cutting zone, and produced a better surface finish compared to the AWJC process. The increase in the hardness of the CAAWJC kerf wall surface caused a restriction on the severe scratches, thereby enabling the kerf wall cut surface with a smooth cutting region by the shearing of thin layer of the target material. This result confirms the erosion process on aluminium

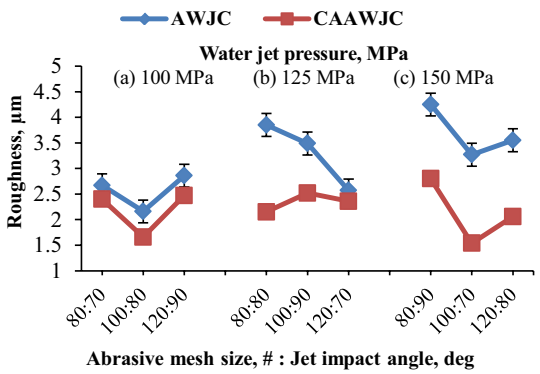

Fig. 9 Variation of surface roughness under different experimental conditions, **a** 100 MPa, **b** 125 MPa, **c** 150 MPa

Table 5 Variation of surface roughness values under AWJC and CAAWJC conditions

Ex. No	P/MPa	MS/#	JIA/(°)	AWJC Avg. R_a (µm)	CAAWJC Avg. R_a (µm)	% of Reduction
1	100	80	70	2.67	2.40	10
2	100	100	80	2.16	1.66	23
3	100	120	90	2.86	2.47	14
4	125	80	80	3.85	2.15	44
5	125	100	90	3.49	2.52	28
6	125	120	70	2.57	2.36	08
7	150	80	90	4.25	2.80	34
8	150	100	70	3.27	1.54	53
9	150	120	80	3.55	2.06	42

alloy as no more serious than erosion at room temperature. Achievement of roughness of a smaller degree seen was possible through a comparison between the various levels of combination in the CAAWJC process with the combined effect of the abrasive water jet impact angle of 70° and an abrasive mesh size #100 along with a water jet pressure of 150 MPa. The lower R_a was found to be 1.54 µm. A lower water jet pressure and abrasive water jet impact angle of 80° produce a lower cutting force, causing a smooth surface finish. This happens when medium coarse (#100) abrasive particles impact the target material during employment of the AWJC process. However, the combined effect of an abrasive water jet impact angle of 90° with an abrasive mesh size of #80 generated a poor surface finish on the top kerf wall cut surface due to the critical action of erosion that took place during the machining of the aluminium alloy. In the CAAWJC process, the fine abrasive mesh size of #120 produced a rough surface at a water jet pressure of 150 MPa and water jet impact angle of 80° was employed. However, this was lower than what was seen in the AWJC process. This was due to the offer of a fine erosion debris process by the cryogenic cutting process attributed to the retention of the size and the shape of the abrasives. This could cause better work material surface quality through an uniform cutting of grains. It confirms that physical geometry of abrasives plays a vital role for improving surface quality under abrasive technique [40]. The results showed, cryogenic cooling as a dominating factor for obtaining a better surface finish in AA5083-H32 aluminium alloy. Finally, it is concluded that, surface roughness in the CAAWJC process got reduced by 8–53% compared to the AWJC process.

3.5 Effect Of LN_2 Cooling on Surface Topography

In order to assess the surface characteristics of AWJC and CAAWJC processes on the top kerf wall cutting region (3 mm from the top kerf wall cut surface), 2D roughness profile and 3D surface topography were carried out, and this is shown in Figs. 10 and 11.

Figure 10a, b show more peaks and valleys in the roughness profile and 3D surface topography as the result of a severe impact, and deep traces on the kerf wall cut surface. It is caused by the ductility of the target material, high impulse of the abrasive particles, and this deformation in the AWJC process. As a result, the surface roughness value was found to be 3.85 µm and the maxium peak to valley height (referred to as Pt in Figs. 10a and 11a in the roughness profile was 22.2 µm. The occurrence of this particular result was due to the cutting deformation caused by a fractured coarse abrasive grain, showing the presence of deep and long wear tracks (brightness of the SEM image) at the top kerf wall surface, as shown in Fig. 10c.

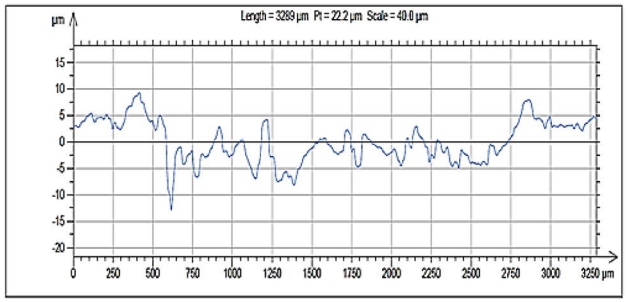

(a)

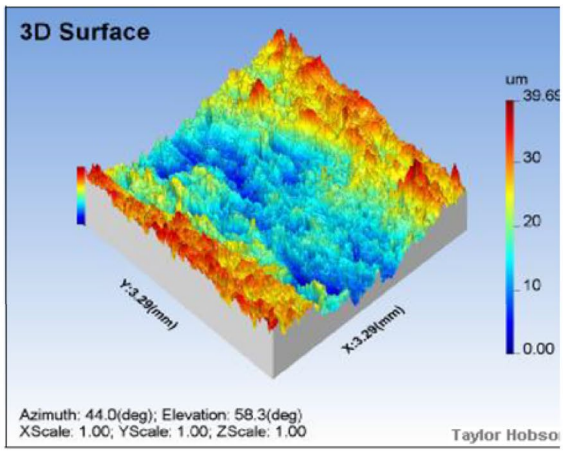

(b)

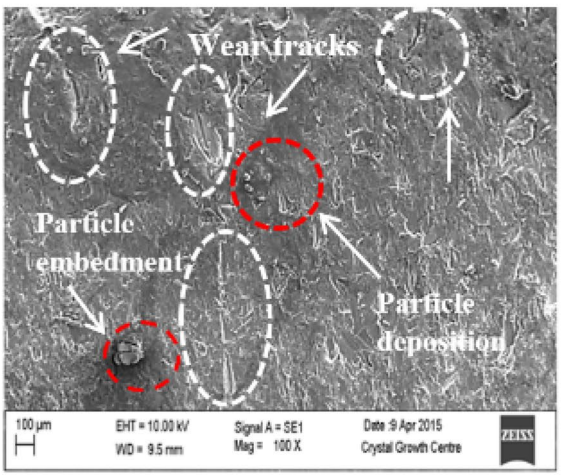

(c)

Fig. 10 Surface topography of abrasive water jet machined surfaces. **a** 2D roughness profile, **b** 3D surface, **c** SEM micrograph of the cut surface

Figure 11a, b, show only a small variation in the 3D surface profile while the roughness value was found to be 1.27 µm. Despite the impact of high impulse of abrasive particles impact with the target material, the CAAWJC process is more susceptible to reduction in ductility, and increase in hardness, thereby facilitating smooth surface finish, and

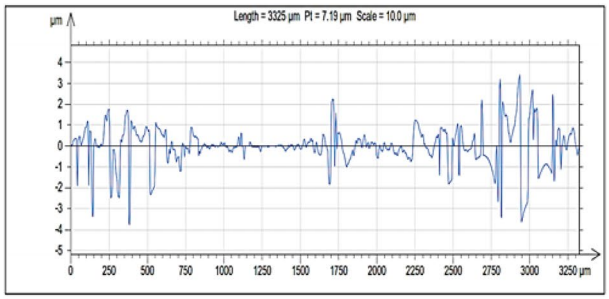

(a)

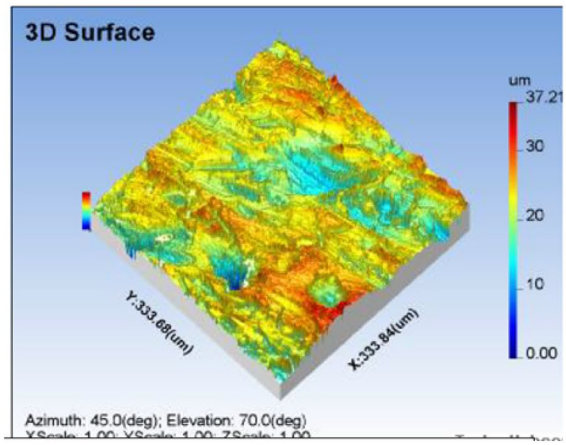

(b)

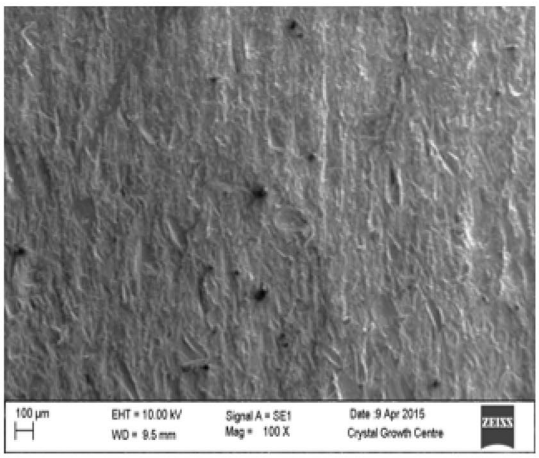

(c)

Fig. 11 Surface Topography of cryogenic assisted abrasive water jet machined surfaces, **a** 2D roughness profile, **b** 3D surface, **c** SEM micrograph of the cut surface

reducing the number of deep traces on the kerf wall surface as well as adhesion of particles at the top cutting region, as shown in Fig. 11c. The result was confirmed by the value of Pt, which is found to be 7.19 µm only. Due to the pouring of LN_2 in the cutting zone, caused prolonged sharpening of abrasive particles involved with effective shearing action,

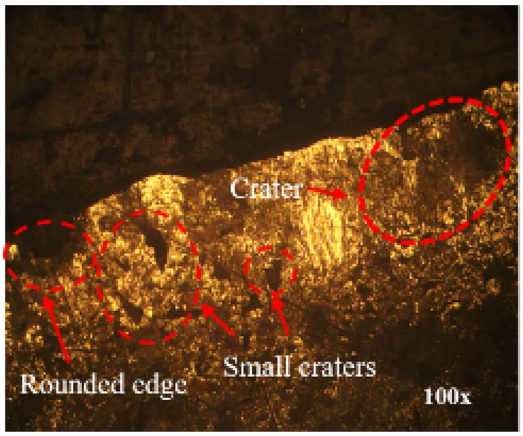

(a)

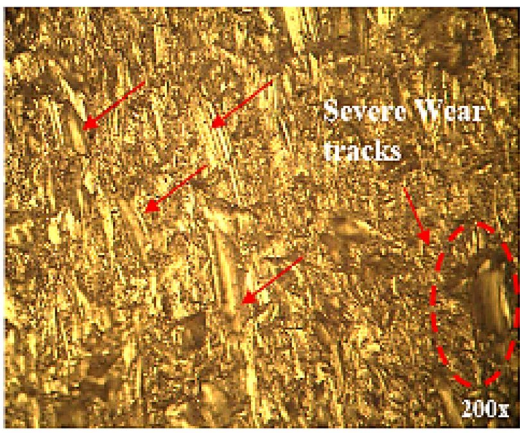

(b)

Fig. 12 Microstructure of AWJC surfaces

and restrictions on the chances of the occurrence of plastic deformation in the target material.

3.6 Effect Of LN_2 Cooling on Microstructure

In this study, an erosion surface analysis was carried out on AA 5083-H32 aluminium alloy using the optical microscopy. The effects of application and non-application of LN_2 cooling on the cut surfaces are shown in Figs. 12 and 13. In the AWJC process, erosion occurred in the cutting and deformation wear mode, in the top cutting region, usually referred to as a damaged region. The damaged region was observed through craters and rounded corners in the top kerf wall cut surface as shown in Fig. 12a, b. This was the result of using plastic deformation of material caused by severe bombardment of coarse abrasive particles at a jet impact angle of 90°. There was also the formation of small craters by embedded particles in the kerf wall cut surface.

Wear tracks were also present as a consequence of particle disintegration with a critical kinetic energy of the AWJ,

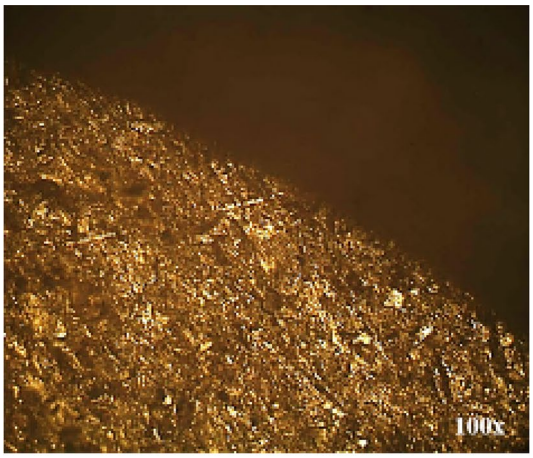

(a)

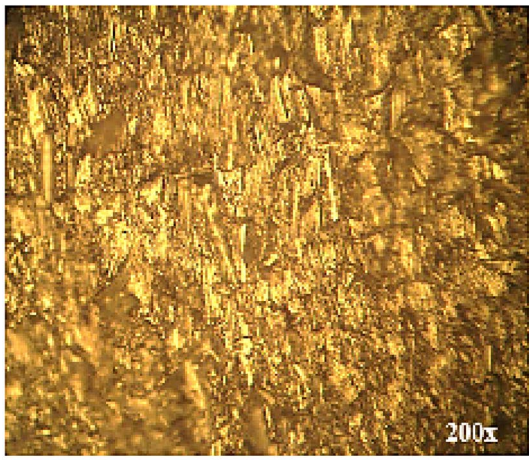

(b)

Fig. 13 Microstructure of CAAWJC surfaces

in which each particle had the minimum threshold energy for improvement in the cutting action of the work material. These results were attributed to the effect of abrasive water jet impact angle of 90° and the abrasive mesh size of #80. These cutting conditions gave rise to a high impulse of the abrasive particles impact with the top kerf wall cut surface. The random orientation of wear tracks in AWJC was seen. This constituted the distribution of the abrasive particles that generated more wear tracks with a non-uniform width. This non-uniform width of the wear tracks was produced as a result of the size and shape of the fracture and fragmentation of the abrasives. Wear tracks of a smaller number were present in the CAAWJC process in the traverse direction of the jet than in the AWJC process, as shown in Fig. 13a, b. This was due to the absence of any craters. There was increase in the hardness of the material caused by the rapid cooling of LN_2 jet, enabling the cut surface to withstand the bombardment of coarse abrasive particles with a reduction in particle embedding in the cutting zone. This facilitates getting a better surface even at the top kerf wall cut surface when LN_2 jet cooling was used.

Figure 14a–e shows the microstructure of the target material under three different conditions, namely the base material, AWJC, and CAAWJC. In AWJC, the grains are randomly oriented and elongated in the initial cutting zone, due to the generation of a possible volume of heat by the abrasive water jet impact angle of 90° and abrasive mesh size #80, combined with a higher water jet pressure. The average cutting zone temperature for the cutting conditions is shown in Fig. 15.

The measurements were taken at a water jet pressure of 150 MPa. The microstructure consists of an eutectic network of Mg_2Al_3 (white) in a matrix of aluminium rich solid solution (dark) in received condition, is shown in Fig. 14a. The micro structure was found at the jet entry of the target material. The temperature was measured at the jet entry of the target material which could be the effect on the grain structure at the cutting zone. A comparison of microstructure revealed, the AWJC kerf wall cut surface having a continuous rich network of β phase (Mg_2Al_3) formed along the grain boundaries. This parameter setting developed heat in the cutting zone during the AWJC process in the range of 55–65 °C, and was recorded by the IR thermometer. Despite being away from the surface, the temperature affected the grain structure which could be due to the property of material and cutting conditions. Because, it is susceptible to modify its structure and properties when exposed to temperature more than 50 °C. This temperature was the result of possible heat generation in the cutting zone at jet impact angle of 90° and abrasive mesh size of #80. This combination offered a high impulse to abrasive particles at the cutting zone. This increased the diffusion of Mg to the grain boundaries, and yielded richer β (thickening) phase surrounding the matrix of the aluminium solid solution, is shown in Fig. 14b. However, no other change in the microstructure was observed. This was due to the less processing time of the target material. In contrast, the microstructure of the abrasive water jet impact angle of 70°, and the abrasive mesh size of #100 indicated a smaller continuity rich network of β phase along the grain boundaries, is shown in Fig. 14d. Of all cutting conditions of CAAWJC kerf wall cut surfaces, a slight continuous intermetallic phase was found without an appreciable quantity of Mg_2Al_3 in a matrix of aluminium rich solid solution, as shown in Fig. 14c, e. This happened as a consequence of the reduction in diffusion at low temperature by LN_2 jet cooling, and the structure appears to retain the parent material microstructure.

Also, the temperature in the CAAWJC zone was observed to be in the range of − 25.6 to − 50 °C. At some points, the temperature was found to be lower than − 50 °C rendering measurement by IR thermometer rather difficult. Further, the percentage of Mg content in the matrix

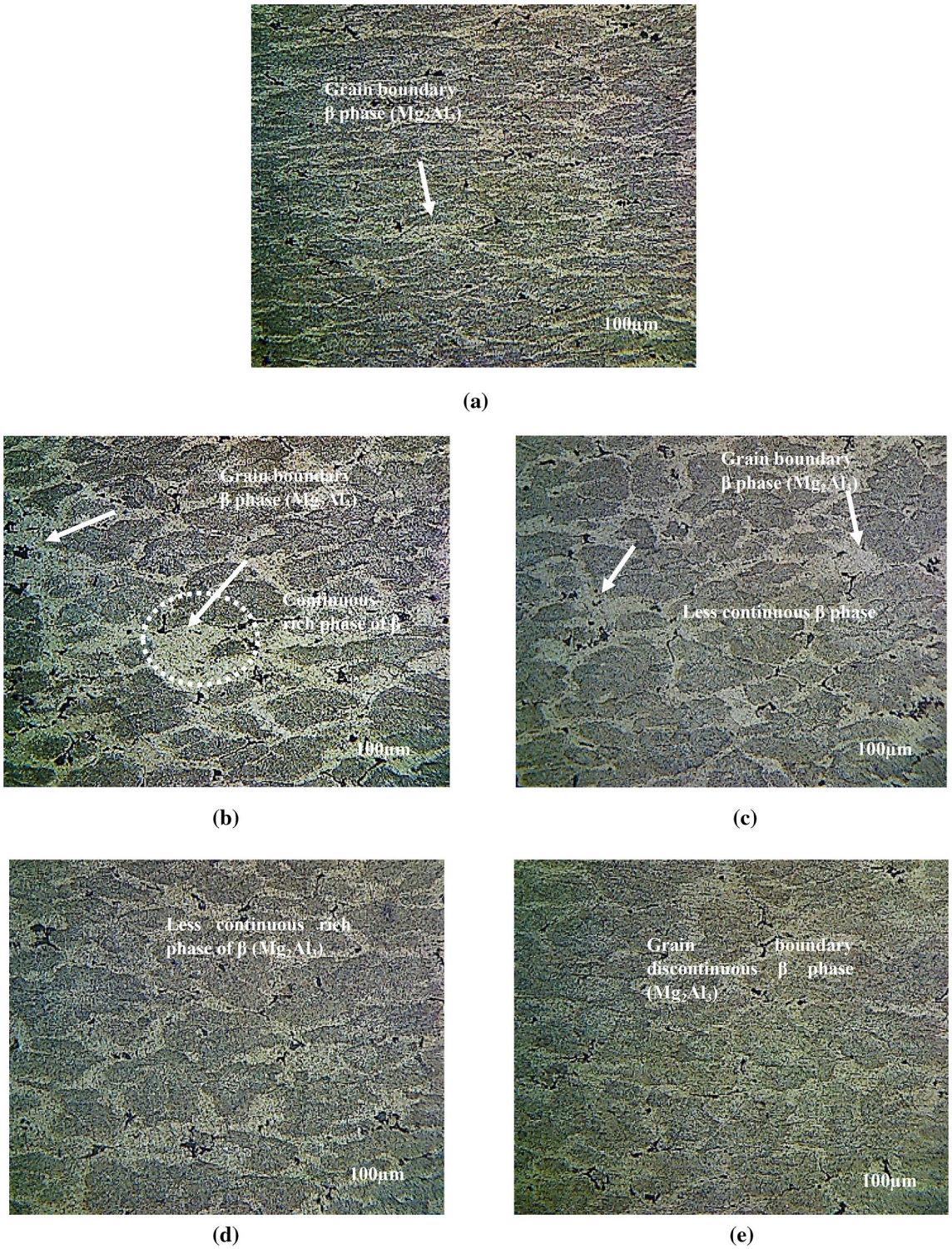

Fig. 14 Microstructure of cut surfaces, **a** base material-as received, **b** AWJC-P: 150 MPa; MS: #80; JIA: 90°, **c** CAAWJC-P: 150 MPa; MS: #80; JIA: 90°, **d** AWJC-P: 150 MPa; MS: #100; JIA: 70°, **e** CAAWJC-P: 150 MPa; MS: #100; JIA: 70°

of solid solution (dark phase) was quantified by using EDS as shown in Fig. 16. The average area measured in the machined surface was 1.5 mm^2. In the AWJC and CAAWJC processes, the EDS analysis was carried out at a water jet pressure of 150 MPa, abrasive mesh size of #80, and abrasive water jet impact angle of 90°. It indicated

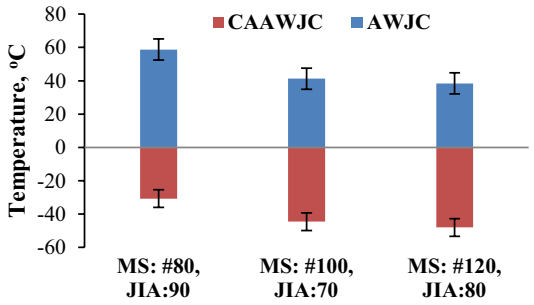

Fig. 15 Variation in average cutting zone temperature under AWJC and CAAWJC conditions

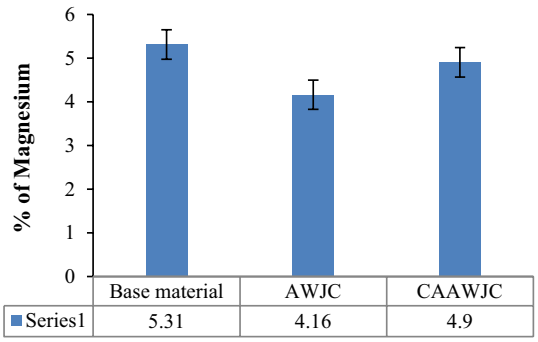

Fig. 16 Percentage of magnesium content

Table 6 Micro hardness of the cut surfaces under AWJC and CAAWJC

Distance (mm)	AWJC, $HV_{0.1kg}$	CAAWJC, $HV_{0.1kg}$
1	76.7	175.3
2	80.4	172.7
3	77.1	150.5
4	73.3	151.9
5	70.6	117.2
6	68.3	116.7

a smaller percentage in the AWJC kerf wall cut surface of Mg over the CAAWJC process. This happened as an excess amount of Mg (> 3%) in a matrix of aluminium rich solid solution to form the β phase particles along the grain boundaries after a shorter exposure period of temperature more than 50 °C. As a result, there was a reduction in the matrix of the solid solution. Table 6 shows the micro hardness values of AWJC and CAAWJC cut surfaces for the water jet pressure of 150 MPa, abrasive mesh size of #80 and abrasive water jet impact angle of 90° in the cutting of AA5083-H32 aluminium alloy.

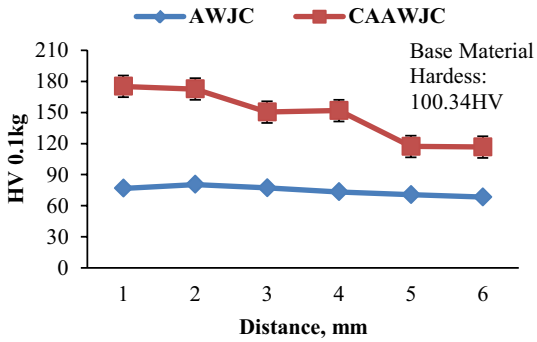

Fig. 17 Variation in micro hardness at different locations

Figure 17 shows increase in the hardness at the distance of 1–6 mm from the top cut surface. This is attributed to the effect of LN_2 cooling, that has made significant changes in the top cutting zone. However, the hardness in the abrasive particle and reduction in particle embedding compensate the machining of harder region in the work material with more efficient. In AWJC process, the high thermal conductivity of the aluminium alloy developed a possible heat at the impact region, and this heat was rapidly conducted into the uncutting regions. This resulted in a reduction in the cooling effect of the jet during an increase in DOP and a consequent decrease in the hardness in the inner cutting regions at a defined depth [41, 42]. Unlike the AWJC process, the CAAWJC process has produced higher hardness with a distance of 6 mm from the top kerf wall cut surface. This occurred due to the removal of heat, and minimal deformation in the cutting zone by LN_2 jet. After exceeding this distance, changes in hardness of the cutting zone were similar to the AWJC process to be expected.

3.7 Effect Of LN_2 Cooling on Abrasive Particle Contamination

Figures 18 and 19 show the effect of abrasive particle contamination in the AWJC and CAAWJC conditions. It is characterised by using SEM with the EDS analysis. This analysis confirmed embedding of some amount of silicon particles in the initial cutting region of the cut surfaces, as silicon was the only element which was not present in the base material composition, as shown in Fig. 20.

In this study, the particle contamination was measured at 3 mm from the top of the cut surface, and the measurement was carried out at a water jet pressure of 150 MPa, abrasive mesh size of #80 and abrasive water jet impact angle of 90°. Figure 18 indicates the production of a large number of silicon particles by AWJC embedded in the top kerf wall cut surface. Also, seen in Fig. 10c, is the particle severely embedded along with the deposition of few abrasives particles are encircled by red colour in the micrograph. This is

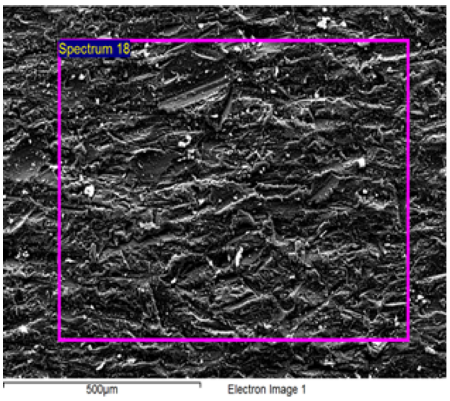

(a)

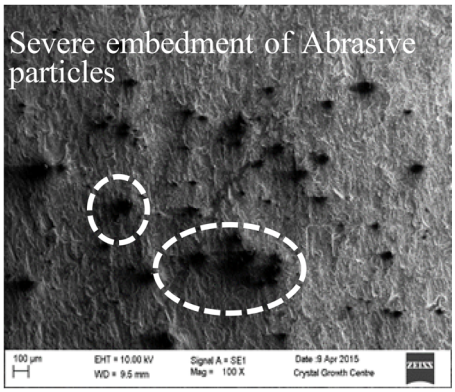

(b)

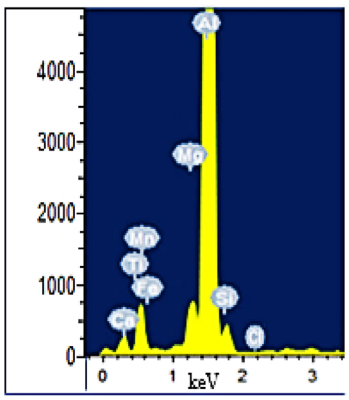

(c)

Fig. 18 Abrasive particle contamination at AWJC cut surface, **a** SE image, **b** SEM image, **c** EDS spectra

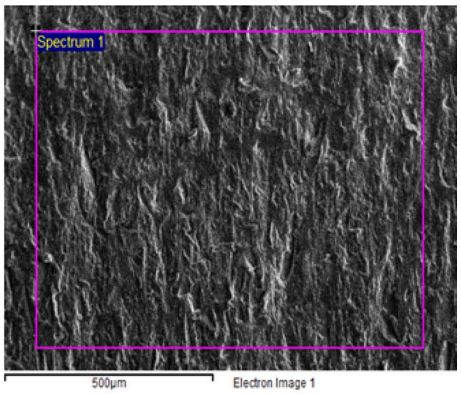

(a)

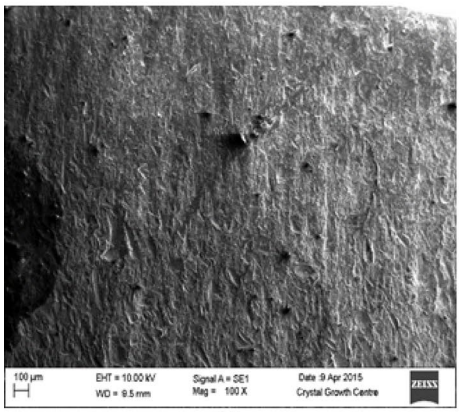

(b)

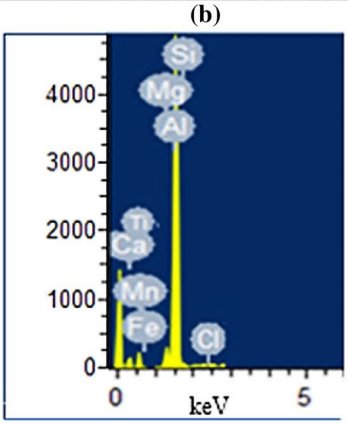

(c)

Fig. 19 Abrasive particle contamination at CAAWJC cut surface, **a** SE image, **b** SEM image, **c** EDS spectra

a corollary of the condition of the target material surface being soft or a lower hardness. The occurrence of abrasive contamination was also due to the high impulse of abrasive particles produced by a jet impact angle of 90°. This contamination produces severe problems with the other operations on these surfaces, such as welding, coating, grinding [43]. However, these particles were drastically reduced in the initial cutting zone of the CAAWJC process, as seen in Fig. 19, because LN_2 cooling reduces particle embedding in the kerf wall cut surfaces, due to the increase in hardness of the cutting zone. An increase in the hardness of the cutting zone resists the abrasive debris embedded in the top kerf wall cut surface. As a result, abrasive debris subsequently passes on to the uncutting region for a more DOP.

Table 7 shows the weight percentage of the silicon present in the cut surfaces. Reduction in the particle contamination of the CAAWJC process by 56.33% was seen while compared to the AWJC. This observation indicated an

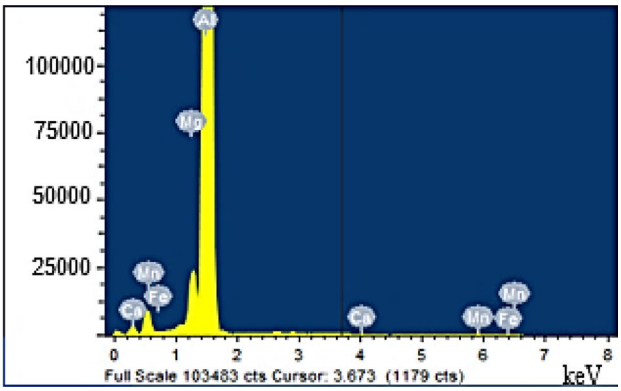

Fig. 20 Base material EDS spectra (before cutting)

Table 7 Percentage of silicon content in the cut surfaces

S. no.	Cutting conditions	% of silicon weight
1.	AWJC	8.52
2.	CAAWJC	3.72

improvement in the cutting performance of the CAAWJC through LN_2 jet cooling, achieving a better surface quality with less contamination. The presence of chlorine (Cl) on the cut surfaces was seen. This was due to the inherent characteristics of the water jet cutting process. However, the Cl content was very low at about 100–200 particles as shown in Figs. 18c and 19c, which did not cause any degradation on the surface characteristics of the material.

4 Conclusions

In this study, conventional abrasive water jet cutting and cryogenic assisted abrasive water jet cutting were carried out on AA5083-H32 aluminium alloy. The major conclusions drawn are given below.

1. In the cryogenic jet cutting operations, the depth of penetration improved by 4–32% over the conventional jet cutting process, due to the reduction in particle embedding in the kerf wall zone.
2. The use of LN_2 jet cooling in the cutting process improved material removal rate in the range of 2–56%. Possible modifications (fine debris/micro cutting) in the erosion process of the target material at low temperature caused an increase in the erosion capability of the abrasive water jet.
3. LN_2 jet cooling produced a reduction of about 2–21% in the taper ratio compared to the jet cutting process at room temperature.
4. The cryogenic assisted abrasive water jet cutting process was found to produce 8–53% less surface roughness compared to the conventional process. A better surface finish was produced by LN_2 jet cooling with support from the fine erosion process in the cutting zone.
5. The cut surface under the cryogenic jet cutting process generated a less deep wear tracks, and peaks and valleys. It was caused by an efficient micro cutting, which occurred through reduction in ductility and, increase in hardness of the cutting zone by LN_2 jet.
6. There was a significant thickening of the β phase (Mg_2Al_3) under the cryogenic jet cutting process. This was confirmed by the quantification of magnesium content in the kerf wall cut surfaces.
7. In the conventional abrasive water jet process, the heat generated in the primary impact zone leads to reduction in hardness. This happens as a result of the generation of peak temperature at abrasive water jet impact angle of 90°.
8. The abrasive particle contamination is greatly reduced by 56% with the help of LN_2 cooling.

Even though above performance results were obtained by cryogenic assisted jet cutting approach, the manual operation of cryogenic nozzle technique was embraced in the present study. In future, it can be developed by an automation of cryogenic nozzle with jet cutting head for the process and performance improvements.

Acknowledgements The authors acknowledge the Head, Department of Production Technology, Madras Institute of Technology (MIT) campus, Anna University, Chennai-44, for providing the experimental facilities to conduct the research work.

Funding The authors would like to express their sincere thanks to the Council of Scientific and Industrial Research (CSIR), Government of India, New Delhi, for providing the research fund under the scheme of Senior Research Fellowship (Grant file no. 0.9/468(479)/2014-EMR-I).

Compliance with ethical standards

Conflict of interest On behalf of all authors, the corresponding author states that there is no conflict of interest.

References

1. Folkes, J. (2009). Waterjet—An innovative tool for manufacturing. *Journal of Materials Processing Technology, 209*(20), 6181–6189.
2. Momber, A., & Kovacevic, R. (1998). *Principles of Abrasive Water Jet Machining*. London: Springer-Verlag.

3. Hashish, M. (1998). Visualisation of the abrasive-waterjet cutting process. *Experimental Mechanics, 28*, 159–168.
4. Patel, D., & Tandon, P. (2015). Experimental Investigations of thermally enhanced abrasive water jet machining of hard-to-machine metals. *CIRP Journal of Manufacturing Science and Technology, 10*, 92–101.
5. Kanthababu, M., & Chetty, O. V. K. (2003). A study on recycling of abrasives in abrasive waterjet machining. *Wear, 254*(7), 763–773.
6. Kanthababu, M., & Chetty, O. V. K. (2006). A study on the use of single mesh size abrasives in abrasive waterjet machining. *International Journal of Advanced Manufacturing Technology, 29*(5), 532–540.
7. Yuvaraj, N., & Kumar, M. P. (2017). Investigation of process parameters influence in AWJ cutting of D2 steel. *Materials and Manufacturing Processes, 32*(2), 151–161.
8. Yuvaraj, N., & Kumar, M. P. (2017). Surface integrity studies on abrasive water jet cutting of AISI D2 steel. *Materials and Manufacturing Processes, 32*(2), 162–170.
9. Yuvaraj, N., & Kumar, M. P. (2017). Study and evaluation of abrasive water jet cutting performance on AA5083-H32 aluminium alloy by varying the jet impingement angles with different abrasive mesh sizes. *Machining Science and Technology, 21*(3), 385–415.
10. Wang, J., Kuriyagawa, T., & Huang, C. Z. (2003). An experimental study to enhance the cutting performance in abrasive waterjet machining. *Machining Science and Technology, 7*(2), 191–207.
11. Boud, F., Murray, J. W., Loo, L. F., Clare, A. T., & Kinnell, P. K. (2014). Soluble abrasives for waterjet machining. *Materials and Manufacturing Processes, 29*(11–12), 1346–1352.
12. Park, K. H., Suhaimi, M. A., Yang, G. D., Lee, D. Y., Lee, S. W., & Kwon, P. (2017). Milling of titanium alloy with cryogenic cooling and minimum quantity lubrication (MQL). *International Journal of Precision Engineering and Manufacturing, 18*(1), 5–14.
13. Umbrello, D., Micari, F., & Jawahir, I. S. (2012). The effects of cryogenic cooling on surface integrity in hard machining: A comparison with dry machining. *CIRP Annals, 61*, 103–106.
14. Pereira, O., Rodríguez, A., Barreiro, J., Fernández-Abia, A.I., de Lacalle, L.N.L. (2017) Nozzle design for combined use of MQL and cryogenic gas in machining. *International Journal of Precision Engineering and Manufacturing-Green Technology*, *4*(1), 87–95.
15. Dhananchezian, M., Kumar, M. P., & Sornakumar, T. (2011). Cryogenic turning of AISI 304 stainless steel with modified tungsten carbide tool inserts. *Materials and Manufacturing Processes, 26*, 781–785.
16. Ravi, S., & Kumar, M. P. (2012). Experimental investigation of cryogenic cooling in milling of AISI D3 tool steel. *Materials and Manufacturing Processes, 27*, 1017–1021.
17. Manimaran, G., & Kumar, M. P. (2013). Effect of cryogenic cooling and sol–gel alumina wheel on grinding performance of AISI 316 stainless steel. *Archives of Civil and Mechanical Engineering, 13*(3), 304–312.
18. Truchot, P., Mellinger, P., & Duchamp, R. (1991) Development of a cryogenic water jet technique for bio material process applications. In: Proceedings of the 6th American Water Jet Conference, USA.
19. Gradeen, A. G., Spelt, J. K., & Papini, M. (2012). Cryogenic abrasive jet machining of polydimethylsiloxane at different temperatures. *Wear, 274–275*, 335–336.
20. Getu, H., Spelt, J. K., & Papini, M. (2011). Thermal analysis of cryogenically assisted abrasive jet micro machining of PDMS. *International Journal of Machine Tools and Manufacture, 61*(9), 721–730.
21. Gardeen, A. G., Papini, M., & Spelt, J. K. (2014). The effect of temperature on the cryogenic abrasive jet micro-machining of polytetrafluoroethylene, high carbon steel and polydimethylsiloxane. *Wear, 317*, 170–178.
22. Urbanovich, L. I., Kramchenkov, E. M., & Chunosov, Y. N. (1992). Investigation of low temperature gas-abrasive erosion. *Soviet Journal of Friction and Wear, 13*, 80–83.
23. Getu, H., Spelt, J. K., & Papini, M. (2008). Cryogenically assisted abrasive jet micromachining of polymers. *Journal of Micromechanics and Microengineering, 18*, 1–8.
24. Spur, G., Uhlmann, E., & Elbing, F. (1999). Dry-ice blasting for cleaning: process, optimization and application. *Wear, 233–235*, 402–411.
25. Liu, H.T., Fang, S., Hibbard, C., & Maloney, J. (1999) Enhancement of ultra-high pressure technology with LN_2 cryogenic jets. In: Proceedings of the 10th American Water Jet Conference on water jet technology, USA.
26. Muju, M. K., & Pathak, A. K. (1998). Abrasive jet machining of glass at low temperature. *Journal of Mechanical Working Technology, 17*, 325–332.
27. Kim, S.K., Lee, D.G.U., Lee, W., Song, O.H.S. (2009) Feasibility study of cryogenic cutting technology by using a computer simulation and manufacture of main components for cryogenic cutting system. *Journal of the Korean Radioactive Waste Society*, *7*(2), 115–125.
28. Kovacevic, R., Hashish, M., Mohan, R., Ramulu, M., Kim, T. J., & Geskin, S. (1997). State of the art of research and development in abrasive waterjet machining. *Journal of Manufacturing Science and Engineering, 119*, 776–785.
29. Yuvaraj, N., & Kumar, M. P. (2016). Cutting of aluminium alloy with abrasive water jet and cryogenic assisted abrasive water jet: A comparative study of the surface integrity approach. *Wear, 362–363*, 18–32.
30. Searless, J. L., Gouma, P. I., & Buchheit, R. G. (2002). Stress corrosion cracking of sensitized AA5083 (Al–4.5Mg–1.0Mn). *Materials Science Forum, 396–402*, 1437–1442.
31. Popovic, M., & Romhanji, E. (2008). Characterization of microstructural changes in an Al6.8wt%Mg alloy by electrical resistivity measurements. *Materials Science and Engineering A, 492*, 460–467.
32. Brosi, J. K., & Lewandowski, J. J. (2010). Delamination of a sensitized commercial Al–Mg alloy during fatigue crack growth. *Scripta Materialia, 63*, 799–802.
33. Li, F., Xiang, D., Qin, Y., Pond, R. B., Jr., & Slusarski, K. (2011). Measurements of degree of sensitization (DoS) in aluminum alloys using EMAT ultrasound. *Ultrasonics, 51*, 561–570.
34. Totten, G. E., & Mackenzie, S. D. (2003). *Handbook of Aluminium Physical Metallurgy and Processes*. New York and Basel: Marcel Dekker Incorporation.
35. Srinivas, S. and Ramesh Babu, N. (2012) Penetration ability of abrasive waterjets in cutting of aluminium–silicon carbide particulate metal matrix composites. *Machining Science and Technology*, *16*, 337–354.
36. Kovacevic, R. (1991). Surface texture in abrasive water jet cutting. *Journal of Manufacturing Systems, 10*, 32–40.
37. Karakurt, I., Aydin, G., & Aydiner, K. (2012). An experimental study on the depth of cut of granite in abrasive waterjet cutting. *Materials and Manufacturing Processes, 27*, 538–544.
38. Zhao, W., & Guo, C. (2014). Topography and microstructure of the cutting surface machined with abrasive waterjet. *International Journal of Advanced Manufacturing Technology, 73*, 941–947.
39. Cheng, K., & Huo, D. (2013). *Micro Cutting: Fundamentals and Applications*. Chichester: Wiley.
40. McGeough, J. A. (2002). *Micromachining of Engineering Materials* (pp. 85–123). New York: Marcel Dekker Publisher.
41. Ohadi, M. M., Ansari, A. I., & Hashish, M. (1992). Thermal distributions in the workpiece during cutting with an abrasive

waterjet. *Journal of Manufacturing Science and Engineering, 114*(1), 67–73.
42. Kovacevic, R., Mohan, R., & Beardsley, H. E. (1996). Monitoring of thermal energy distribution in abrasive water jet cutting using infrared thermography. *Journal of Manufacturing Science and Engineering, 118*, 555–563.
43. Patel, K. J. (2004). Quantitative evaluation of abrasive contamination in ductile material during abrasive water jet machining and minimizing with a nozzle head oscillation technique. *International Journal of Machine Tools and Manufacture, 44*, 1125–1132.

Yuvaraj Natarajan currently working as an Assistant Professor (Research) in the Department of Mechanical Engineering at Vel Tech Rangarajan Dr. Sagunthala R&D Institute of Science and Technology, Chennai. He completed his M.E. and Ph.D. in the Department of Mechanical Engineering at CEG campus, Anna University, Chennai. And, he received his B.Tech. degree from University College of Engineering – BIT campus, Anna University, Trichy, India. His research interests are metal cutting, cryogenics, water jet peening, surface characterization and MCDM techniques.

Pradeep Kumar Murugasen is currently serving as Professor in the Department of Mechanical Engineering at College of Engineering Guindy Campus, Anna University Chennai, India. He received his Ph.D and M.E from Anna University, Chennai. He has almost 15 years of teaching and research experience in the field of manufacturing processes. He has published many research articles in International and National Journals. His research interests are cryogenic machining, application of FEM in machining and micromachining.

Lenin Raj Sundarajan is pursuing Ph.D. (FT) in the Department of Production Engineering at Madras Institute of Technology, Anna University, Chennai, India. He received his B.E and M.E in Production Engineering from MIT campus, Anna University, Chennai. His current areas of research include abrasive water jet machining of metals and non-metals.

Rajadurai Arunachalam working as Professor in the Department of Production Engineering at Madras Institute of Technology, Anna University, Chennai, India. He received his Ph.D (Metallurgy) and M.E. (Metallurgy) from Indian Institute of Science, Bangalore. He has published more than 200 articles in various journals and conferences. His research interests are finite element analysis, metal cutting, composites and material characterization.